

Controlling edge dynamics in complex networks

Tamás Nepusz^{1,2} and Tamás Vicsek^{1,2,*}

December 30, 2011

Abstract

The interaction of distinct units in physical, social, biological and technological systems naturally gives rise to complex network structures. Networks have constantly been in the focus of research for the last decade, with considerable advances in the description of their structural and dynamical properties. However, much less effort has been devoted to studying the controllability of the dynamics taking place on them. Here we introduce and evaluate a dynamical process defined on the edges of a network, and demonstrate that the controllability properties of this process significantly differ from simple nodal dynamics. Evaluation of real-world networks indicates that most of them are more controllable than their randomized counterparts. We also find that transcriptional regulatory networks are particularly easy to control. Analytic calculations show that networks with scale-free degree distributions have better controllability properties than uncorrelated networks, and positively correlated in- and out-degrees enhance the controllability of the proposed dynamics.

The last decade has witnessed an explosive growth of interest in the descriptive analysis of complex natural and technological systems that permeate many aspects of everyday life [3, 11, 42]. Research in network science has mostly been focused on measuring [6, 8, 62], modeling [28, 44] and decomposing [22, 43, 47] network representations of existing natural phenomena in order to deepen our understanding of the underlying systems. Considerably less attention has been dedicated to the various types of network dynamics [19, 34, 46, 52] and even less to the problem of controllability [33, 53, 63], i.e. determining the conditions under which the dynamics of a network can be driven from any initial state to any desired final state within finite time [26, 32, 59, 60].

Structural controllability [31] has been proposed recently as a framework for studying the controllability properties of directed complex networks [32]. In this framework, a linear time-invariant nodal dynamics is assumed on the network, governed by the following equation:

$$\dot{\mathbf{x}}(t) = \mathbf{A}\mathbf{x}(t) + \mathbf{B}\mathbf{u}(t) \quad (1)$$

where \mathbf{A} is the transpose of the (weighted) adjacency matrix of the network, $\mathbf{x}(t)$ is a time-dependent vector of the state variables of the nodes, $\mathbf{u}(t)$ is the vector of input signals, and \mathbf{B} is the so-called *input matrix* which defines how the input signals are connected to the

¹Department of Biological Physics, Eötvös Loránd University, Pázmány Péter sétány 1/a, 1117 Budapest, Hungary.

²Statistical and Biological Physics Research Group of the Hungarian Academy of Sciences, Pázmány Péter sétány 1/a, 1117 Budapest, Hungary.

*Corresponding author: vicsek@hal.elte.hu

nodes of the network. The dynamics is said to be *structurally controllable* if there exists a matrix \mathbf{A}^* with the same structure as \mathbf{A} such that the network can be driven from any initial state to any final state by appropriately choosing the input signals $\mathbf{u}(t)$ [31]. Here, structural equivalence of \mathbf{A} and \mathbf{A}^* means that \mathbf{A}^* is not allowed to contain a non-zero entry when the corresponding entry in \mathbf{A} is zero. Structural controllability is a general property in the sense that almost all weight combinations of a given network are controllable if the network is structurally controllable for a given \mathbf{B} [31, 57]. The minimum number of input signals is then determined by finding a maximum matching in the network, i.e. a maximum subset of edges such that each node has at most one inbound and at most one outbound edge from the matching. The number of nodes without inbound edges from the matching is then equal to the number of input signals required for structural controllability [32].

Perhaps the most striking feature of the structural controllability approach to linear nodal dynamics is that input signals tend to control the hubs of the network only indirectly. In addition, real-world networks that seem to have evolved to control an underlying process (such as transcriptional regulatory networks) need many input signals [32]. This is due to the fact that driven nodes (i.e. those which receive an input signal directly) are not able to control their subordinates independently from each other. However, these results apply only for linear nodal dynamics. In this paper, we examine and describe a dynamics that takes place on the edges of the network, and show that this dynamics leads to significantly different controllability properties for the same real-world networks.

1 Switchboard dynamics in complex networks

We study a dynamical process on the edges of a directed complex network $G(V, E)$ as follows. Let $\mathbf{x} = [x_j]$ denote the state vector of the process, where one state variable corresponds to each edge of the network. Let \mathbf{y}_i^- and \mathbf{y}_i^+ be vectors consisting of those x_j values that correspond to the inbound and outbound edges of vertex i , respectively, and let \mathbf{M}_i denote a matrix with the number of rows being equal to the out-degree and the number of columns being equal to the in-degree of vertex i . Furthermore, we assume that the dynamics can be influenced from the environment by adding an offset vector \mathbf{u}_i to the state vector of the outbound edges of any node i . The equations governing the dynamics of the network are then as follows:

$$\dot{\mathbf{y}}_i^+(t) = \mathbf{M}_i \mathbf{y}_i^-(t) - \boldsymbol{\tau}_i \otimes \mathbf{y}_i^+(t) + \sigma_i \mathbf{u}_i(t) \quad (2)$$

where $\boldsymbol{\tau}_i$ is a vector of damping terms corresponding to the edges in $\mathbf{y}_i^+(t)$, σ_i is 1 if vertex i is a so-called *driver node* and zero otherwise, and \otimes denotes the entry-wise product of two vectors of the same size.

We call the above the *switchboard dynamics* (SBD) since each vertex i acts as a small switchboard-like device mapping the signals of the inbound edges to the outbound edges using a linear operator \mathbf{M}_i , which is called the *mixing* or *switching matrix* from now on. To simplify the equations, state variables and signals like \mathbf{y}_i^+ , \mathbf{y}_i^- and \mathbf{u}_i are implicitly considered as time-dependent, even if the time variable t is omitted. Furthermore, note that for an edge $v \rightarrow w$, exactly one of the coordinates of \mathbf{u}_v affects the state of this edge, therefore we can simply introduce a unified input vector \mathbf{u} where the j th element u_j is simply the component of the offset vectors that affects edge j directly.

In some sense, the SBD provides a simplified representation of the underlying dynamic processes of many real-world networks. For instance, in social communication networks, a

node (i.e. a person) is constantly processing the information received via its inbound edges and makes decisions which are then communicated to other nodes via the outbound edges. The inbound and outbound signals are then represented by the state variables x_j , while the decision process is modeled by the mixing matrices \mathbf{M}_i .

We must also explain the motivation of introducing the offset vectors as a means of controlling the system instead of assuming external input signals. In most networks, one usually can not take control over a single edge as the connections do not always have a physical realization. Therefore, in order to control an edge in a network, one has to take control over the vertex from which the edge originates, and adjust the output vector of the vertex appropriately. This adjustment is represented by the term $\sigma_i \mathbf{u}_i$ for each vertex i . Throughout this paper, we will be interested in determining an optimal control configuration for the SBD of a given network, where optimality is measured by the number of driver nodes $\sigma = \sum_i \sigma_i$.

First, we make a connection between the switchboard dynamics and a standard linear dynamical system by re-writing the equations of the switchboard dynamics (Eq. (2)) in terms of x_i . Note that the derivative of the state of an arbitrary edge j originating in some vertex r and terminating in vertex s depends only on itself and on the states of edges whose head is r . Let us denote this latter set by Γ_j^- , simplifying our dynamical equation to

$$\dot{x}_j = \sum_{k \in \Gamma_j^-} w_{kj} x_k - \tau_j x_j + \sigma_s u_j \quad (3)$$

where w_{kj} is the element in the mixing matrix \mathbf{M}_r of vertex r that corresponds to edge k (as inbound edge) and edge j (as outbound edge), τ_j is the damping term related to edge j , and u_j is equal to the value of the input signal affecting the state variable of edge j . Defining $w_{kj} = 0$ for all $k \notin \Gamma_j^-$ yields

$$\dot{\mathbf{x}} = (\mathbf{W} - \mathbf{T})\mathbf{x} + \mathbf{H}\mathbf{u} \quad (4)$$

where the unknown variables are as follows:

- $\mathbf{W} = [w_{kj}]$ is a matrix where w_{kj} may be nonzero if and only if the head of edge k is the tail of edge j .
- \mathbf{T} is a diagonal matrix with the damping terms of each edge in the main diagonal.
- \mathbf{H} is a diagonal matrix where the j th diagonal element is σ_s if vertex s is the tail of edge j .

Eq. (4) essentially describes a simple linear time-invariant dynamical system of the form $\dot{\mathbf{x}} = \mathbf{A}\mathbf{x} + \mathbf{B}\mathbf{u}$ with the substitution $\mathbf{A} = \mathbf{W} - \mathbf{T}$ and $\mathbf{B} = \mathbf{H}$. It is also easy to see that \mathbf{W} is the adjacency matrix of the *line digraph* $L(G)$ of the original digraph G by definition. The nodes of $L(G)$ thus correspond to the edges of the original network G , and each edge of $L(G)$ represents a length-two directed path of G . An example network G is shown in Figure 1a, and its corresponding line digraph on Figure 1b. The loop edges arising from the damping term $-\mathbf{T}$ in Eq. (2) are omitted from Figures 1b and 1c, partly for sake of clarity, and partly because soon we will demonstrate that such edges do not change the optimal control configuration.

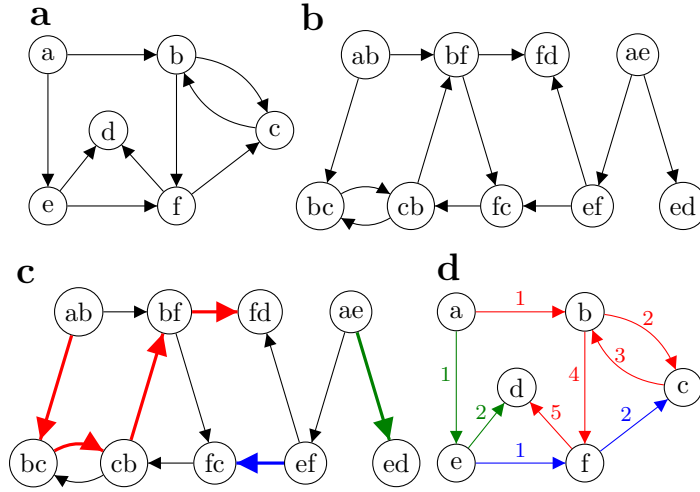


Figure 1: (a) An example network G with six vertices and nine edges. The switchboard dynamics takes place on the edges of the network. (b) The line graph $L(G)$ corresponding to G . A linear time-invariant dynamics on the vertices of this network is equivalent to the switchboard dynamics on G . Node labels refer to the endpoints of the edges in G to which they correspond. (c) Applying the maximum matching theorem to $L(G)$ yields disjoint control paths. (d) The control paths in G , mapped back from $L(G)$. Note how each path in $L(G)$ became an edge-disjoint walk in G . Numbers represent the order in which the edges have to be traversed in the walks. The two driver nodes are a and e since each walk starts from either a or e .

2 Structural controllability of the switchboard dynamics

Applying the maximum matching theorem of Liu et al [32] to $L(G)$ (Figure 1b) gives us a set of control paths and driven nodes in the line digraph (Figure 1c), or equivalently, a set of driven *edges* in the original graph G . Since edges can be controlled only via the offset vectors, the set of driver nodes are given by collecting those vertices that have at least one outbound driven edge. However, note that the maximum matching theorem guarantees only that the number of driven nodes in $L(G)$ will be minimal, and this does not imply that the obtained set of driver nodes in G is also minimal.

Let us now compare the control paths obtained from the maximum matching in the line graph $L(G)$ in Figure 1c with the corresponding control paths in the original graph G in Figure 1d. It can be seen that the maximum matching consists of vertex-disjoint open and closed paths (also called *stems* and *buds*) in $L(G)$, and mapping these paths back to G yields *edge-disjoint* open and closed walks in G . The walks together form a complete cover of the edges of G . Since the first vertex of each stem has to be driven in $L(G)$, the driver nodes in G are those from which the corresponding open edge-disjoint walks originate. Our goal is thus to find a cover that minimizes the number of nodes from which open walks originate in G .

Let us call a vertex v *divergent* if $d_v^+ > d_v^-$, *convergent* if $d_v^+ < d_v^-$, and *balanced* if $d_v^+ = d_v^-$, and let us define a *balanced component* as a connected component consisting solely of balanced vertices and at least one edge. Our key result (which can also be formulated as a theorem) is that the minimum set of driver nodes required to control the SBD on a network $G(V, E)$ can be determined by selecting the divergent vertices of G and one arbitrary vertex

from each balanced component. The formal proof is given in the Appendix.

The above theorem has two important implications. First, it explains why we are safe to ignore loop edges in $L(G)$: a loop edge of a vertex in G increases both its in-degree and its out-degree by one, thus a divergent vertex stays divergent, and a non-divergent vertex stays non-divergent. Second, the theorem shows that the number of driver nodes required to control the SBD is almost completely determined by the joint degree distribution of the network. This is in concordance with the results of Liu et al [32] for the linear time-invariant nodal dynamics.

3 Controllability of real networks

We have determined the set of driver nodes under the switchboard dynamics for 38 real networks classified into 11 categories and compared the fraction of driver nodes n_D with the model of Liu et al [32] and with its expected value after different types of randomizations (see Table 1). A striking difference between the switchboard dynamics and the model of Liu et al [32] can be seen for two classes of networks. Regulatory networks such as the transcriptional regulatory network of *E.coli* (TRN-EC-2 [37]) and *S.cerevisiae* (TRN-Yeast-1 [7], TRN-Yeast-2 [37]) and the ownership network of US telecommunications and media corporations (Ownership-USCorp [45]) turned out to be well-controllable under the switchboard dynamics but they are very hard to control in the linear nodal dynamics. This can be explained by the fundamental difference between the two models. In the linear nodal dynamics, a driven node may not influence its subordinates independently of each other, thus the presence of out-hubs in a network degrades its controllability significantly. In the switchboard dynamics, out-hubs behave the opposite way, allowing one to control many state variables with a single out-hub. It follows that driver nodes *prefer* out-hubs in the SBD, while they are shown to *avoid* hubs in the linear nodal dynamics. Therefore, hubs have an important role not only in maintaining the connectivity of a network in case of random failures [5, 15, 24] and containing epidemic spreading [50, 51], but they also make it possible to control the network efficiently with a smaller number of driver nodes.

The other class of networks with the largest difference between the two models is the case of intra-organizational networks [17, 23, 41]. In the model used by Liu et al, all these networks can be controlled by at most three nodes. On closer examination, it turns out that 75%-80% of the connections in each of these networks is reciprocal, i.e. an edge exists between vertices A and B in both directions. A reciprocal edge pair can easily form a bud in a maximum matching, requiring no driver node on its own, therefore high reciprocity in a network always implies a low fraction of driver nodes in the linear nodal dynamics, while this is not necessarily true for the SBD.

Comparing the fraction of driver nodes for the SBD with the randomized variants reveals that in most cases, the fraction of driver nodes required to control a random Erdős–Rényi network [12, 20] of the same size is larger than the fraction of driver nodes for the real-world network, suggesting that the structure of these networks is at least partially optimized for controllability. Notable exceptions are the electronic circuits [37], the neural network of *C.elegans* [1, 62], most of the World Wide Web networks [2, 4, 28, 48], and the intra-organizational networks [17, 23, 41]. Preserving the in- and out-degree distributions (but not the joint distribution) brings the fraction of driver nodes closer to the observed one after randomization, and keeping the joint degree distribution makes the fraction of driver nodes

Table 1: Controllability properties of the real networks analysed in this paper

Type	#	Name	Nodes	Edges	n_D^{SBD}	n_D^{Liu}	n_D^{ER}	n_D^{Degree}
Regulatory	1.	Ownership-USCorp	7,253	6,726	0.160	0.820	0.339	0.085
	2.	TRN-EC-2	418	519	0.222	0.751	0.366	0.148
	3.	TRN-Yeast-1	4,441	12,873	0.034	0.965	0.415	0.033
	4.	TRN-Yeast-2	688	1,079	0.177	0.821	0.381	0.137
Trust	5.	College*	32	96	0.344	0.188	0.418	0.315
	6.	Epinions*	75,888	508,837	0.336	0.549	0.445	0.448
	7.	Prison*	67	182	0.403	0.134	0.411	0.451
	8.	Slashdot*	82,168	948,464	0.323	0.045	0.458	0.392
	9.	WikiVote*	7,115	103,689	0.281	0.666	0.463	0.620
Food web	10.	Grassland	88	137	0.318	0.523	0.381	0.297
	11.	Little Rock	183	2,494	0.639	0.541	0.463	0.649
	12.	Seagrass	49	226	0.449	0.265	0.436	0.433
	13.	Ythan	135	601	0.304	0.511	0.432	0.337
Metabolic	14.	<i>C. elegans</i>	1,173	2,864	0.182	0.302	0.409	0.309
	15.	<i>E. coli</i>	2,275	5,763	0.182	0.382	0.409	0.309
	16.	<i>S. cerevisiae</i>	1,511	3,833	0.185	0.329	0.409	0.313
Electronic circuits	17.	s208a	122	189	0.451	0.238	0.381	0.431
	18.	s420a	252	399	0.456	0.234	0.385	0.440
	19.	s838a	512	819	0.459	0.232	0.381	0.442
Neuronal and brain	20.	<i>C. elegans</i>	297	2,359	0.549	0.165	0.449	0.499
	21.	Macaque	45	463	0.333	0.022	0.446	0.457
Citation	22.	arXiv-HepPh*	34,546	421,578	0.356	0.232	0.459	0.577
	23.	arXiv-HepTh*	27,770	352,807	0.359	0.216	0.460	0.569
WWW	24.	Google	15,763	171,206	0.670	0.337	0.457	0.612
	25.	Polblogs	1,490	19,090	0.509	0.471	0.460	0.501
	26.	nd.edu	325,729	1,497,134	0.271	0.677	0.433	0.301
	27.	stanford.edu	281,904	2,312,497	0.665	0.317	0.450	0.653
Internet	28.	p2p-1	10,876	39,994	0.334	0.552	0.425	0.344
	29.	p2p-2	8,846	31,839	0.344	0.578	0.423	0.344
	30.	p2p-3	8,717	31,525	0.343	0.577	0.424	0.344
Social communication	31.	Twitter* [†]	41.7×10^6	1.47×10^9	0.402	–	0.476	0.434
	32.	UCIOnline	1,899	20,296	0.216	0.323	0.456	0.375
	33.	WikiTalk	2,394,385	5,021,410	0.022	0.968	0.399	0.026
Organizational	34.	Consulting*	46	879	0.522	0.043	0.458	0.460
	35.	Freemans-1*	34	645	0.412	0.088	0.441	0.476
	36.	Freemans-2*	34	830	0.588	0.029	0.439	0.465
	37.	Manufacturing*	77	2,228	0.597	0.013	0.468	0.424
	38.	University*	81	817	0.519	0.012	0.451	0.532

Notations are as follows: fraction of driver nodes under the switchboard dynamics (n_D^{SBD}) and the simple nodal dynamics [32] (n_D^{Liu}); fraction of driver nodes under the switchboard dynamics in randomized networks using the Erdős–Rényi model (n_D^{ER}) and the degree-preserving configuration model (n_D^{Degree}). Note that this latter model does not preserve the joint degree distribution. Results for null models are averaged from 100 randomizations. Networks where the edges were reversed compared to the original publication are marked by * (see Appendix, section C.1). Results calculated directly from the degree distribution (i.e. not taking into account balanced components) are marked by †.

practically the same up to a difference of ± 0.002 in the networks we have studied, confirming that the effect of balanced components on the fraction of driver nodes is indeed negligible for large real-world networks. Edge deletion experiments (see Appendix) also indicate that the optimal control configurations in the studied networks are robust to single link failures as the networks mostly remain controllable with the same number of driver nodes after the removal of a single edge.

4 Analytical results for model networks

The dependence of n_D on the joint degree distribution allows us to derive analytical formulae for the expected fraction of driver nodes for a wide variety of model networks (see Appendix for the exact derivations). For Erdős–Rényi digraphs [12, 20] with n vertices and an edge probability of p , n_D is given as follows:

$$n_D^{\text{ER}} = \frac{1}{2} - \frac{e^{-2\langle k \rangle}}{2} I_0(2\langle k \rangle) \quad (5)$$

where $\langle k \rangle = np$ is the average in- and out-degree and $I_\alpha(x)$ is the modified Bessel function of the first kind. The function converges rapidly to 0.5 as $\langle k \rangle$ increases. Similar results are obtained for graphs with independent exponential in- and out-degree distributions $Ce^{-k/\kappa}$ where $\kappa = 1/\log \frac{1+\langle k \rangle}{\langle k \rangle}$:

$$n_D^{\text{exp}} = \frac{\langle k \rangle}{2\langle k \rangle + 1} \quad (6)$$

which also approaches 0.5 rapidly as $\langle k \rangle \rightarrow \infty$ (Figure 2a). For power-law distributed digraphs [8, 13] with $\mathbf{P}(d_v^+ = k) = \mathbf{P}(d_v^- = k) = Ck^{-\gamma}e^{-k/\kappa}$, n_D is given by

$$n_D^{\text{power}} = \frac{1}{2} - \frac{\text{Li}_{2\gamma}(e^{-2/\kappa})}{2\text{Li}_\gamma(e^{-1/\kappa})^2} \quad (7)$$

where $\text{Li}_s(z)$ is the base s polylogarithm function. As $\kappa \rightarrow \infty$, this converges to

$$n_D^{\text{power}} = \frac{1}{2} - \frac{\zeta(2\gamma)}{2\zeta(\gamma)^2} \quad (8)$$

(where $\zeta(x)$ is the Riemann zeta function) in the absence of any exponential cutoff (Figure 2b). The Appendix also contains the analytical treatment of k -regular networks.

It is worthwhile to compare these analytical results with that of Liu et al [32], who have found that the fraction of driver nodes n_D decreases for both Erdős–Rényi and scale-free networks as $\langle k \rangle \rightarrow \infty$, while these networks behave the opposite way under the SBD. For $\langle k \rangle \rightarrow \infty$, the fraction of driver nodes tends to $1/2$ for Erdős–Rényi networks and to $1/2 - \zeta(2\gamma)/(2\zeta(\gamma)^2)$ for scale-free networks. The consequence is that denser networks are harder to control (as expected by our intuition), and that scale-free networks with a given $\langle k \rangle$ are *easier* to control than an Erdős–Rényi network with the same average degree. This can partly be attributed to the higher frequency of short loops [10] in scale-free networks: these loops can be covered by closed walks and do not require extra driver nodes.

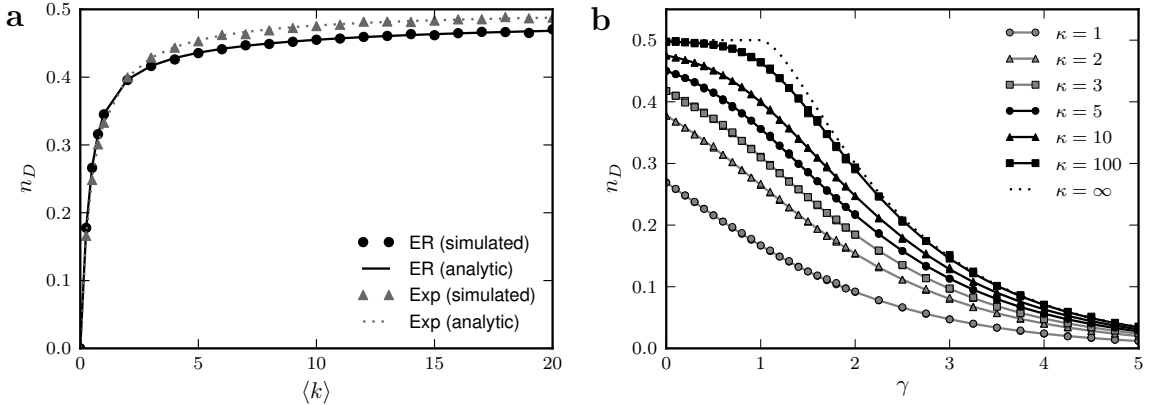


Figure 2: **(a)** Expected fraction of driver nodes n_D in Erdős–Rényi (ER) and exponential (Exp) networks as a function of the average degree $\langle k \rangle$. **(b)** Expected fraction of driver nodes n_D in scale-free networks with exponential cutoff as function of the exponent γ of the degree distribution, for different cutoff values κ . On both panels, symbols denote the results of simulations on networks with 10^5 nodes, solid lines correspond to the analytical results.

5 The effect of degree correlations

Our analytical results assumed that the in-degree and the out-degree of a node is uncorrelated, which was true for all of the model networks we have studied. However, one-point degree correlations in real networks are significantly different from zero [9]. To study how such correlations affect the fraction of driver nodes, we have performed simulations on Erdős–Rényi networks and scale-free networks with an exponential cutoff and varied the correlation as follows. First, we generated an instance of the network model with $n = 10^5$ nodes and calculated the in- and out-degree sequences. These instances were uncorrelated since neither the Erdős–Rényi model nor the configuration model (which we have used to generate scale-free networks) introduces correlations between the in- and out-degree of the same node. Next, while keeping the in-degree sequence intact, we started swapping elements in the out-degree sequence randomly such that only those swaps were performed which increased the correlation. The process was continued until we were not able to increase the correlation any more in the last t steps (where $t = 10^4$ in our simulations). A similar greedy algorithm was executed from the original degree sequences in the opposite direction, performing swaps only if it decreased the correlation, terminating when it was not possible to decrease the correlation any more in the last t steps. The fraction of driver nodes n_D was then calculated in the original configuration and whenever the absolute difference of the calculated in- and out-degree correlation between the last examined state and the current state became larger than 0.01.

The results are depicted in Figures 3a and 3b, both of which clearly show a general trend: increasing the correlation between the in- and out-degrees decreases the fraction of driver nodes. Negative one-point correlations yield a higher fraction of driver nodes since these networks are very unlikely to contain balanced nodes: a vertex either has a high in-degree and a low out-degree or a high out-degree and a low in-degree. In other words, negative correlations indicate a clear separation of responsibilities between the nodes of the network: divergent nodes are strongly divergent with a large difference between the out-degree and

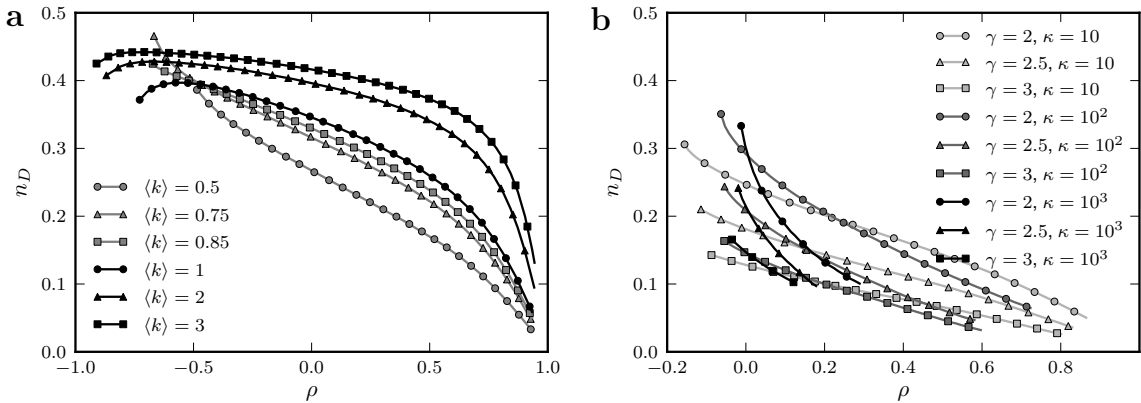


Figure 3: **(a)** Fraction of driver nodes n_D in Erdős-Rényi (ER) networks with different average degree $\langle k \rangle$ as a function of in- and out-degree correlation (ρ). **(b)** Fraction of driver nodes n_D in scale-free networks with different exponents γ as a function of in- and out-degree correlation (ρ). On both panels, every fifth data point is marked by a symbol. Each data point was obtained by averaging at least 20 different realizations of the network model; error bars were omitted as they were smaller than the symbols. Note that it is very hard to introduce negative degree correlations in the case of scale-free networks and none of our test runs managed to decrease the correlation below -0.2.

the in-degree, while convergent nodes are strongly convergent. Positive correlations indicate that nodes often represent complex decision processes which map a high-dimensional input space into a similarly high-dimensional output space. Strong positive correlations also yield networks with a higher number of short loops [9], which can then be covered by closed walks that do not require driver nodes on their own.

6 Conclusions

We have presented a linear time-invariant dynamical model where state variables correspond to the edges of a directed complex network, and the nodes of the network act as linear operators that map state variables of inbound edges to outbound edges. We have demonstrated that the minimum number of driver nodes for such systems is largely determined by the joint degree distribution of the network. A comprehensive survey of 38 real-world networks showed that transcriptional regulatory networks are well-controllable with a small number of driver nodes under the switchboard dynamics, and that most real-world networks are easier to control than random Erdős-Rényi networks with the same number of nodes and edges. This is very different from the findings of Liu et al [32] who have reported a high fraction of driver nodes under linear nodal dynamics on regulatory networks and that randomized Erdős-Rényi networks are easier to control than the real-world ones. The results suggest that one should choose the dynamical model carefully before studying the controllability properties of a real-world network as it may affect the results to a very large extent.

The behaviour of the nodal and edge dynamics is markedly different in highly hierarchical, tree-like networks where the presence of central out-hubs rapidly increase the required number of driver nodes for the linear nodal dynamics of Liu et al, while the same out-hubs

allow efficient control of many subordinate nodes and thus decrease the required number of driver nodes in the switchboard dynamics. Such hierarchies are ubiquitous in nature and society, from scales as small as gene regulatory networks [7, 37], through leader-follower relationships of flocking pigeons [39], to the large-scale organization of some man-made social structures like the Wikipedia talk network [29] or the ownership network of US media and telecommunications corporations [45]. The presence or absence of hierarchy thus seems to be an important contributing factor of the controllability properties of large dynamical systems.

As it happens so often in scientific research, the framework we have presented raises more questions than answers. For instance, it is yet unknown how the switchboard dynamics would behave in the presence of noise or nonlinearity, or in cases when it is enough to control only a subset of the state variables (output controllability) and only ensure that the uncontrollable ones have stable dynamics (stabilizability). However, as we have shown, even the first steps along our approach could be used to deepen our understanding of the origins of controllability of real-world networks.

Acknowledgments

This research was supported by the EU ERC COLLMOT project. We are grateful to Enys Mones for useful discussions.

Appendices

A Structural controllability

A.1 Controllability conditions

A continuous linear dynamical system of the form $\dot{\mathbf{x}} = \mathbf{A}\mathbf{x}$, $\mathbf{A} \in \mathbb{R}^{n \times n}$ is said to be *controllable* by a set of piecewise continuous input signals \mathbf{u} if we are able to drive the state vector \mathbf{x} from any arbitrary initial state to any given state in finite time, assuming that the input signals are injected to the linear system according to the following dynamical equation:

$$\dot{\mathbf{x}} = \mathbf{A}\mathbf{x} + \mathbf{B}\mathbf{u} \tag{9}$$

where $\mathbf{B} \in \mathbb{R}^{n \times m}$ is a matrix that describes how the input signals affect the derivatives of the state variables. \mathbf{A} is usually called the *state matrix* and \mathbf{B} the *control matrix*. Note that the structure of \mathbf{B} is not constrained in any way; one can connect any of the input signals to any of the state variables.

The *Kalman rank condition* states that the system is controllable if and only if the *controllability matrix* $[\mathbf{B} \ \mathbf{A}\mathbf{B} \ \mathbf{A}^2\mathbf{B} \ \dots \ \mathbf{A}^{n-1}\mathbf{B}]$ has rank n , where n is the number of state variables [26, 60]. However, the rank condition is not constructive since it does not tell us how to find an appropriate \mathbf{B} for a given \mathbf{A} (preferably with a minimum number of columns), and even testing the Kalman rank condition is computationally expensive and numerically unstable for large n . Due to these difficulties, control theorists turned to the concept of *structural controllability*, first introduced by Lin in his seminal paper [31].

In the structural controllability framework, one assumes that the matrices \mathbf{A} and \mathbf{B} contain two kinds of elements: fixed zeros and free parameters. The free parameters of the matrices

may assume any real value and are independent of each other. A system with state matrix \mathbf{A} and control matrix \mathbf{B} is then structurally controllable if it is possible to set the free parameters of the matrices in a way that the system becomes controllable in the usual sense. It can also be shown that if a system is structurally controllable, then it is also controllable for all parameter values except a set of combinations with zero Lebesgue measure [31, 57]; in other words, structural controllability is a general property of the system and it implies controllability for almost all combinations of the free parameters.

Sufficient and necessary conditions for the structural controllability of linear time-invariant dynamical systems with known state and control matrices $\mathbf{A} = [a_{ij}]$ and $\mathbf{B} = [b_{ij}]$ were given earlier in the literature [38, 54]. The graph-theoretic formulation of the condition is given as follows. Let $G(V, E)$ the graph representation of the dynamic system, where $V = \{x_1, x_2, \dots, x_n, u_1, u_2, \dots, u_m\}$, $E = E_A \cup E_B$, $E_A = \{(x_i, x_j) | a_{ji} \neq 0\}$ and $E_B = \{(u_i, x_j) | b_{ji} \neq 0\}$. Similarly, let $G^*(V^*, E^*)$ be the so-called *bipartite graph representation* of the system, where $V^* = V_R \cup V_C \cup V_U$, $V_R = \{x_1^+, x_2^+, \dots, x_n^+\}$, $V_C = \{x_1^-, x_2^-, \dots, x_n^-\}$, $V_U = \{u_1, u_2, \dots, u_m\}$, $E^* = E_A^* \cup E_B^*$, $E_A^* = \{(x_i^+, x_j^-) | a_{ji} \neq 0\}$ and $E_B^* = \{(u_i, x_j^-) | b_{ji} \neq 0\}$. Note that there exists a bijection between E and E^* : (x_i, x_j) in E is equivalent to (x_i^+, x_j^-) in E^* , and (u_i, x_j) in E is equivalent to (u_i, x_j^-) in E^* . The system is then structurally controllable if and only if the following two conditions hold:

1. For all $v \in V$, v is reachable from at least one of $\{u_1, u_2, \dots, u_m\}$ via directed paths in G . This is called the *reachability* condition.
2. G^* contains n independent edges, where a set of edges is *independent* if every vertex in V^* is incident on at most one of the edges.

The bijection between E and E^* means that the set of independent edges satisfying the above conditions selects n edges from E such that each vertex $v \in V$ is incident on at most one inbound and at most one outbound selected edge. For sake of simplicity and also to conform with the terminology introduced earlier by Liu et al [32], we will call a set of edges satisfying this condition a *matching*¹, vertices with inbound selected edges *matched* and vertices without such edges *unmatched*. Note that all input vertices u_i are unmatched since they have no inbound edges, and no ordinary vertex v_i will be unmatched because 1) we have selected n independent edges, 2) there are exactly n ordinary vertices, 3) we know that none of the input vertices are matched, and 4) a selected edge can make only one vertex matched.

The selected edges form vertex-disjoint directed paths and cycles in G . The directed paths are called *stems* and they always originate from one of the input vertices u_i (since the first vertex of a stem is unmatched and only the input vertices are unmatched). The directed cycles are called *buds*. Stems and buds together form the set of *control paths*, since we can think about them in an informal way as principal routes along which control signals propagate in the system. A peculiar property of buds is that they do not require a separate control signal: if any vertex of a bud is adjacent to the vertex of a stem, then the stem itself will be responsible for providing the appropriate input to the vertices of the bud as well. Note that due to the reachability condition (see page 11) there can be no bud in the system that is

¹The definition of “matching” in this manuscript is not to be confused with matchings on *undirected* graphs, where it is required that the selected edges share no common vertices. In this manuscript, “matching” always refers to a directed matching as defined above.

not adjacent to any of the stems since each vertex is accessible from at least one input vertex, and each input vertex is the root of one of the stems.

The above conditions can only be used to check whether the system is structurally controllable once the control matrix \mathbf{B} is known. In a recent paper [32], Liu et al have proven the *maximum matching theorem*, which states that the minimum number of input signals required to control a system represented by its state matrix \mathbf{A} can be determined by finding a maximum matching in \mathbf{A} or a maximum set of independent edges in the bipartite representation of \mathbf{A} (assuming no input vertices), and then counting the number of unmatched vertices. The maximum matching theorem also constructs the matrix \mathbf{B} in a way that the bipartite representation of the system with state matrix \mathbf{A} and control matrix \mathbf{B} will satisfy the above conditions for structural controllability. This is achieved by connecting an input signal to every unmatched vertex of the graph to form one stem for each such vertex, and also connecting these input signals to any buds that are not adjacent to stems in order to satisfy the reachability condition. The nodes of the original network that are connected directly to one of the input signals are called *driven nodes*, and the nodes of the input signals are called *driver nodes*.

It is important to emphasize the distinction between driver and driven nodes, since the difference between them may be arbitrarily large. The reason for this is that one driver node may drive more than one driven node. To show that this is not just a rare theoretical possibility, we refer the Reader to a recently published manuscript of Cowan et al [16], where the authors argue that the dynamic equations of real networks usually include a damping term for each state variable. These damping terms ensure that the system returns to some ground state in the absence of external stimuli. The damping terms are represented by nonzero diagonal elements in \mathbf{A} and by self-loops in the network representation of the system. When all the nodes in the network are equipped with self-loops, a trivial maximum matching can be obtained by selecting the self-loops only, thus constructing n buds. According to the maximum matching theorem of Liu et al, the system then requires a single driver node only, which will be connected to all the nodes of the network. Thus, the number of *driver* nodes will be 1 and the number of *driven* nodes will be n , attaining the maximum possible difference of $n - 1$. Furthermore, the theorem then states that *every* real-world network with such self-loops can be driven by a single input signal.

The distinction between driver and driven nodes is fundamental in the simple linear time-invariant nodal dynamics assumed by Liu et al, but not in the switchboard dynamics. In the switchboard dynamics, driver nodes are *internal* to the system: these are the nodes whose mixing matrix M_i is controlled in order to drive the state variables of the edges into the desired state. Choosing all the self-loops in the line graph $L(G)$ of the switchboard dynamics would simply promote every node of the original network with at least one outbound edge to a driver node. Later on in Section A.2, we will prove that this is not necessarily an optimal solution and also show a linear-time algorithm that selects the optimal driver node configuration.

A.2 Proof of our key result

For sake of clarity, we repeat some definitions from the main part of the manuscript here.

Definition 1 (Divergent vertex). *A vertex v in a digraph $G(V, E)$ is divergent if $d_v^+ > d_v^-$, where d_v^+ is the out-degree and d_v^- is the in-degree of the vertex.*

Definition 2 (Convergent vertex). *A vertex v in a digraph $G(V, E)$ is convergent if $d_v^+ < d_v^-$.*

Definition 3 (Balanced vertex). A vertex v in a digraph $G(V, E)$ is balanced if $d_v^+ = d_v^-$.

Definition 4 (Balanced component). A connected component $C \subseteq V$ in a digraph $G(V, E)$ is a balanced component if v is balanced for every $v \in C$ and C contains at least one edge.

We will also need a few more definitions and lemmas:

Definition 5 (Edge-disjoint walk). An edge-disjoint walk of a digraph $G(V, E)$ is a sequence of vertices v_0, v_1, \dots, v_n such that $v_i \rightarrow v_{i+1}$ is a member of E for every $0 \leq i < n$ and each such edge appears in the walk only once. Such a walk is open if $v_0 \neq v_n$ and closed otherwise.

Lemma 1. For every connected component $C \subseteq V$ of a digraph $G(V, E)$, exactly one of the following three statements is true:

1. C contains no edges.
2. C contains at least one convergent and at least one divergent vertex.
3. C is balanced.

Proof. Proving that at most one of the three statements can be true at the same time is trivial and follows from the definitions above. To complete the proof, we must also show that at least one of the statements must always be true. This is done by contradiction. Suppose that there exists a connected component C in some graph $G(V, E)$ for which none of the three statements holds. C then either contains at least one convergent vertex and no divergent vertices, or at least one divergent vertex and no convergent vertices. Both cases are contradictory since the sum of in-degrees in any connected component C must be equal to the sum of out-degrees, and balanced vertices contribute the same amount to both sums. \square

Lemma 2. For every connected component $C \subseteq V$ of a digraph $G(V, E)$ containing at least one edge, one of the following two statements is true:

1. C can be covered by a single closed edge-disjoint walk.
2. C can be covered by a set of open edge-disjoint walks.

Proof. Lemma 1 states that for non-empty connected components, the component is either balanced or contains at least one divergent vertex. If the component is balanced, the in-degree of each vertex is equal to the out-degree, hence it is always possible to construct an Eulerian circuit in it using Hierholzer's algorithm [21]. An Eulerian circuit is a closed edge-disjoint walk by definition, thus C satisfies case 1.

If C is not balanced, there exists at least one divergent vertex in C . We then construct a set of open walks using the following algorithm:

1. Select an arbitrary divergent vertex v . If there are no divergent vertices in the component, go to step 4.
2. Build a walk by following an arbitrary outgoing edge of the current vertex repeatedly until the walk gets stuck in a vertex w , while making sure that each edge is included in the walk only once.

3. Store the walk, remove its edges from the component and go back to step 1. Note that the walk is always open ($v \neq w$) since v has more outbound edges than inbound ones, hence the walk cannot get stuck in v .
4. At this step, there are no more divergent vertices in C . By Lemma 1, this implies that all the vertices are balanced. Since C may have fallen apart into multiple connected components after the edge removals, construct an Eulerian circuit for each sub-component of C and store it as a closed walk.

The above algorithm provides us with a cover of C with edge-disjoint open and closed walks. However, note that each closed walk can be eliminated by finding an open walk with which it shares a vertex v and joining them together in a larger open walk which traverses the original open walk from the beginning until it arrives at v , then traverses the closed walk, and resumes the original open walk at v again. Repeating this procedure for every closed walk in the cover provides us with a final cover containing open walks only. This corresponds to case 2 in the lemma and concludes our proof. \square

Our key result is then as follows:

Theorem 1. *The minimum set of driver nodes required to control the switchboard dynamics on a network $G(V, E)$ can be determined by selecting the divergent vertices of G and one arbitrary vertex from each balanced component.*

Proof. The proof will proceed as follows. First, we provide an algorithm which constructs an edge cover in G such that each open walk originates in a divergent node and each balanced component is covered by a single closed walk, giving an upper bound on the minimum number of driver nodes. Next, we show that every divergent node must be driven in G in any control configuration, and that one arbitrary vertex from each balanced component must also be driven, providing a lower bound on the minimum number of driver nodes. We then show that the upper and lower bounds coincide, therefore our algorithm is optimal.

We have already shown in the main part of this manuscript that the switchboard dynamics on G is equivalent to a linear time-invariant dynamics on the nodes $L(G)$, for which a set of driver and driven nodes can be determined using the maximum matching theorem of Liu et al [32]. The maximum matching theorem states that a given matching in $L(G)^*$ yields a set of stems (directed vertex-disjoint paths) and buds (directed vertex-disjoint cycles) in $L(G)$, and the roots of the stems (i.e. the first vertices in the order of traversal) have to be controlled by external signals². Buds do not require separate driver nodes because they are either adjacent to a stem (and thus use the signal from the stem) or one of the nodes in the bud is connected to an already existing input signal directly. The driven nodes will be the roots of the stems and an arbitrarily chosen vertex in each bud that is not adjacent to a stem.

Each non-loop edge in the line digraph $L(G)$ corresponds to a length-two path in G . This implies that each stem in $L(G)$ corresponds to a concatenation of length-two paths, yielding an edge-disjoint walk on G , which may contain the same vertex multiple times but may not traverse the same edge twice. Similarly, buds not containing a loop edge in $L(G)$ correspond to edge-disjoint closed walks on G , and buds consisting of a single loop edge in $L(G)$ yield a single open path of length 1 in G . Since each vertex in $L(G)$ participates in either a stem

²In case of a non-maximum matching, some of the nodes have no incident edges selected in the matching; these nodes can be considered as stems on their own.

or a bud (but not both at the same time), mapping the stems and buds in $L(G)$ back to G provides us with a cover of G using edge-disjoint closed and open walks. Note that the mapping is injective: an edge-disjoint walk in G can also be mapped back uniquely to a stem or a bud in $L(G)$. Therefore, a matching in $L(G)$ is completely equivalent to a cover of G with edge-disjoint walks, and we are free to work with either of them.

A possible cover of edge-disjoint walks can be obtained using the algorithm described in Lemma 2. Such a cover creates a closed walk for every balanced component and a set of open walks for every non-balanced component. Mapping the walks to $L(G)$ gives us a set of stems and buds:

- Closed walks will become buds without loop edges in $L(G)$.
- Open walks with at least two edges become stems in $L(G)$.
- Open walks with a single edge will correspond to the appropriate loop edge in $L(G)$, thus becoming a bud with a single loop edge.

Together, these stems and buds form a set of control paths. Each stem requires an input signal, hence the first vertex of each open walk in G (i.e. every divergent vertex) will have to be driven. Since closed walks occur exclusively within balanced components, and each balanced component contains only one closed walk, the buds corresponding to them will not be adjacent to any of the stems in $L(G)$, hence they will also have to be connected to some input signal directly. The only way we are allowed to achieve this in case of the switchboard dynamics is to promote one of the nodes in the bud to a driver node. Therefore, one driver node will be required for every balanced component and for every divergent node of G . We have thus obtained an upper bound on the number of driver nodes in G . To prove that the algorithm in Lemma 2 is optimal and conclude the proof, we will show that this is also a lower bound.

Assume that there exists a complete cover of the edges (i.e. a control configuration) of G and there exists a divergent node v such that v is not a driver node. Since v is not a driver node, there is no open walk originating from it. Let us now consider all the walks v is a part of. Closed walks enter and leave v the same number of times. Since no open walk originates from v , each open walk either enters and leaves v the same number of times, or terminates in v . Therefore, the number of covered inbound edges of v must be equal to or larger than the number of covered outbound edges of v . However, since v is divergent, it has more outbound edges than inbound edges, therefore at least one outbound edge is not covered. This contradicts our assumption that we are working with a complete cover. Therefore, by contradiction, we have shown that every divergent vertex of G must be a driver node in any control configuration.

Due to the reachability condition (see page 11), we must also ensure that there is at least one driver node in every connected component not containing a divergent vertex. Lemma 1 states that every connected component C of G is empty, balanced, or contains at least one convergent vertex. To satisfy the reachability condition, we must therefore promote one of the vertices in every balanced component to a driver node. Therefore, a lower bound on the number of driver nodes in G is the number of divergent nodes plus the number of balanced components of G . Since the lower and upper bounds coincide, our algorithm is optimal. This concludes our proof. \square

Note that the algorithm given above allows one to determine the minimum set of driver nodes for the switchboard dynamics on an arbitrary graph $G(V, E)$ in $O(n+m)$ time (where n is the number of vertices and m is the number of edges): building the edge-disjoint walks takes $O(m)$ time (since each edge has to be evaluated only once), calculating the connected components takes $O(n+m)$, and an additional $O(n)$ step can decide which connected components are balanced.

B Analytical results

In the main part of this manuscript, we have presented analytical formulae for the expected fraction of driver nodes in Erdős–Rényi, exponential and scale-free networks. These formulae are based on the fact that the fraction of driver nodes depends almost completely on the joint degree distribution of the network according to Theorem 1. By neglecting the possible existence of balanced components, the fraction of driver nodes for graphs with a joint degree distribution $\mathbf{P}(d_v^- = i, d_v^+ = j) = p_{ij}$ is simply given by

$$n_D = \sum_{i=0}^{\infty} \sum_{j=i+1}^{\infty} p_{ij} \quad (10)$$

i.e. one simply has to calculate the sum of joint probabilities for cases when the in-degree is smaller than the out-degree. When the in- and out-degrees are uncorrelated and identically distributed (as in all the model networks we have presented in the main part of this manuscript), it is also true that $p_{ij} = p_{ji}$, hence n_D can also be written as

$$n_D = \frac{1 - \sum_{k=0}^{\infty} p_{kk}}{2} \quad (11)$$

i.e. the fraction of driver nodes is equal to half the probability of non-balanced nodes. The formulae presented in the main part of this manuscript are all based on Eq. 11 by substituting the actual degree distribution of the network model in question.

B.1 Erdős–Rényi digraphs

For Erdős–Rényi digraphs with n vertices and an edge probability of p , both the in- and out-degrees follow a Poisson distribution with $\langle k \rangle = np$, hence n_D is given as follows:

$$n_D^{\text{ER}} = \frac{1}{2} \left(1 - \sum_{k=0}^{\infty} \frac{\langle k \rangle^{2k}}{k!k!} e^{-2\langle k \rangle} \right) = \frac{1}{2} \left(1 - e^{-2\langle k \rangle} I_0(2\langle k \rangle) \right) \quad (12)$$

where $I_\alpha(x)$ is the modified Bessel function of the first kind. An equivalent derivation follows from the fact that the difference of the in- and out-degree of a node follows a Skellam distribution [58], thus the probability of balanced nodes is equal to the value of the probability moment function of Skellam($\langle k \rangle, \langle k \rangle$) at $x = 0$.

B.2 Exponential networks

In exponential networks, in-degrees and out-degrees are assumed to be distributed with $\mathbf{P}(d_v^+ = k) = \mathbf{P}(d_v^- = k) = C e^{-k/\kappa}$ where $C = 1 - e^{-1/\kappa}$ and $\kappa = 1/\log \frac{1+\langle k \rangle}{\langle k \rangle}$. The ex-

pected value of n_D then follows from simple algebraic manipulations:

$$n_D^{\text{exp}} = \frac{1}{2} \left(1 - C^2 \sum_{i=0}^{\infty} e^{-2i/\kappa} \right) = \frac{1}{2} \left(1 - C^2 \frac{1}{1 - e^{-2/\kappa}} \right) = \frac{1}{2} \left(1 - \frac{1 - e^{-1/\kappa}}{1 + e^{-1/\kappa}} \right) \quad (13)$$

$$= \frac{e^{-1/\kappa}}{1 + e^{-1/\kappa}} = \frac{\langle k \rangle}{\langle k \rangle + 1} \frac{\langle k \rangle + 1}{2 \langle k \rangle + 1} = \frac{\langle k \rangle}{2 \langle k \rangle + 1} \quad (14)$$

where in the penultimate step we have made use of $e^{-1/\kappa} = \frac{\langle k \rangle}{\langle k \rangle + 1}$.

B.3 Power-law networks

In this case, we distinguish between networks with a power-law-like distribution that has an exponential cutoff of the form $\mathbf{P}(d_v^+ = k) = \mathbf{P}(d_v^- = k) = Ck^{-\gamma}e^{-k/\kappa}$, and pure power-law distributions without a cutoff that follow $\mathbf{P}(d_v^+ = k) = \mathbf{P}(d_v^- = k) = Ck^{-\gamma}$. The exponential cutoff makes it possible to normalize the distribution for a given average degree. We will start with the former case and then show how n_D behaves as the exponential cutoff vanishes (i.e. $\kappa \rightarrow \infty$).

In the general case, n_D is given by

$$n_D^{\text{power}} = \frac{1}{2} \left(1 - C^2 \sum_{i=0}^{\infty} k^{-2\gamma} e^{-2k/\kappa} \right) = \frac{1}{2} \left(1 - C^2 \text{Li}_{2\gamma}(e^{-2/\kappa}) \right) = \frac{1}{2} - \frac{\text{Li}_{2\gamma}(e^{-2/\kappa})}{2 \text{Li}_{\gamma}(e^{-1/\kappa})^2} \quad (15)$$

since we know that $C = \text{Li}_{\gamma}(e^{-1/\kappa})$, where $\text{Li}_s(z)$ is the polylogarithm function. For $z = 1$, the polylogarithm reduces to the Riemann zeta function, yielding

$$n_D^{\text{power}} = \frac{1}{2} - \frac{\zeta(2\gamma)}{2\zeta(\gamma)^2} \quad (16)$$

for pure power-law networks.

B.4 k -regular networks

The three network models presented so far produce balanced components with a very low probability, hence we were safe to ignore such components in our analytical calculations. In this section, we present similar calculations for networks where the in- and out-degree of each vertex is $k/2$ for some even k . These networks consist of balanced nodes only, and the number of driver nodes is given by the number of connected components of the graph containing at least one edge.

Theorem 2. *In a k -regular directed network $G(V, E)$ with n vertices, the number of driver nodes is zero if $k = 0$, one if $k \geq 4$ and the n th harmonic number H_n if $k = 2$.*

Proof. The case of $k = 0$ is trivial: there are no edges to control and hence the fraction of driver nodes is zero. For $k \geq 4$, dropping the arrowheads gives us an undirected k -regular graph where it can be proven that it is almost surely k -connected [12], implying that the original digraph requires only one driver node. For $k = 2$, each vertex has exactly one inbound and one outbound edge, thus the entire graph consists of disjoint directed cycles. By denoting the head of the outbound edge of vertex v by $\pi(v)$, we obtain a permutation π

on the vertices of the graph, and the number of connected components will be given by the number of cycles in π .

Let us call a sequence of elements u_1, u_2, \dots, u_m an m -cycle of π if each u_i is equal to some v_j and it holds that $\pi(u_1) = u_2, \pi(u_2) = u_3, \dots, \pi(u_m) = u_1$. First we prove that the probability of the event that v_1 is a part of an m -cycle is $1/n$. We require that $u_1 = v_1, u_2 = \pi(u_1) \neq v_1, u_3 = \pi(u_2) \neq v_1, \dots, \pi(u_m) = v_1$. Therefore,

$$\mathbf{P}(v_1 \text{ is in an } m\text{-cycle}) = \frac{n-1}{n} \frac{n-2}{n-1} \frac{n-3}{n-2} \dots \frac{n-m}{n-m+1} \frac{1}{n-m} = \frac{1}{n}$$

Of course the above proof applies to every $v_i \in V$. Since each v_i is a part of an m -cycle with probability $1/n$, the expected number of vertices being part of an m -cycle is exactly 1, and since an m -cycle contains m vertices, the expected number of m -cycles is $1/m$. The expected number of cycles of any length \mathcal{E} then follows by a simple summation:

$$\mathcal{E} = \sum_{m=1}^n \frac{1}{m} = H_n$$

This concludes our proof. □

Since H_n scales approximately as $\log n$, the fraction of driver nodes will scale as $\log n/n$ and tend to zero as $n \rightarrow \infty$. k -regular graphs are thus extremely well-controllable in the infinite limit, requiring $O(1)$ driver nodes if $k \neq 2$ and $O(\log n)$ driver nodes if $k = 2$.

C Computational results

C.1 Data sources of real networks

The details of the real-world networks we have studied are presented in Table C.1. Note that the semantics of the switchboard dynamics requires that a directed $A \rightarrow B$ edge represents a direct influence of A on B and not the other way round, hence we had to reverse the edge directions in some of the networks to make it conform to this semantics. For instance, an $A \rightarrow B$ edge in a trust network usually means that A trusts B , hence B has a direct influence on A . For sake of clarity, the table includes the semantics of each edge.

C.2 Robustness of control configurations

To study the robustness of real networks against random control path failures, we have classified each edge according to the change in the number of driver nodes when the edge is removed from the network. We distinguish three cases and accordingly three classes of edges. The removal of a *critical* edge increases the number of driver nodes required to maintain controllability. Conversely, the removal of a so-called *distinguished* edge decreases the number of driver nodes. The remaining edges are called *ordinary* since their removal does not affect the set of driver nodes.

Figure 4 shows the fraction of critical, ordinary and distinguished edges in each studied real network, indicating that most networks possess only a small fraction of critical or distinguished edges, thus exhibiting a high degree of robustness against changes in control configurations due to random edge removals. The two significant exceptions are the electronic circuit networks (s208a, s420a and s838a) [37], which contain a high fraction of distinguished edges, and the metabolic networks [25], where almost half of the edges are critical.

Type	#	Name	n	m		Semantics of $A \rightarrow B$
Regulatory	1.	Ownership-USCorp	7,253	6,726	[45]	A owns B
	2.	TRN-EC-2	418	519	[37]	A regulates B
	3.	TRN-Yeast-1	4,441	12,873	[7]	A regulates B
	4.	TRN-Yeast-2	688	1,079	[37]	A regulates B
Trust	5.	College*	32	96	[36, 61]	A is trusted by B
	6.	Epinions*	75,888	508,837	[55]	A is trusted by B
	7.	Prison*	67	182	[36, 61]	A is trusted by B
	8.	Slashdot*	82,168	948,464	[30]	A is trusted by B
	9.	WikiVote*	7,115	103,689	[29]	A was voted on by B
Food web	10.	Grassland	88	137	[18]	A preys on B
	11.	Little Rock	183	2,494	[35]	A preys on B
	12.	Seagrass	49	226	[14]	A preys on B
	13.	Ythan	135	601	[18]	A preys on B
Metabolic	14.	<i>C. elegans</i>	1,173	2,864	[25]	B is produced from A
	15.	<i>E. coli</i>	2,275	5,763	[25]	B is produced from A
	16.	<i>S. cerevisiae</i>	1,511	3,833	[25]	B is produced from A
Electronic circuits	17.	s208a	122	189	[37]	B is a function of A
	18.	s420a	252	399	[37]	B is a function of A
	19.	s838a	512	819	[37]	B is a function of A
Neuronal and brain	20.	<i>C. elegans</i>	297	2,359	[1, 62]	B is within one synapse or gap junction distance from A
	21.	Macaque	45	463	[40]	Area A is connected to area B
Citation	22.	arXiv-HepPh*	34,546	421,578	[28]	A is cited by B
	23.	arXiv-HepTh*	27,770	352,807	[28]	A is cited by B
WWW	24.	Google	15,763	171,206	[48]	A links to B
	25.	Polblogs	1,490	19,090	[2]	A links to B
	26.	nd.edu	325,729	1,497,134	[4]	A links to B
	27.	stanford.edu	281,904	2,312,497	[28]	A links to B
Internet	28.	p2p-1	10,876	39,994	[28, 56]	A sent messages to B
	29.	p2p-2	8,846	31,839	[28, 56]	A sent messages to B
	30.	p2p-3	8,717	31,525	[28, 56]	A sent messages to B
Social communication	31.	Twitter*	41.7×10^6	1.47×10^9	[27]	A is followed by B
	32.	UCIOnline	1,899	20,296	[49]	A sent emails to B
	33.	WikiTalk	2,394,385	5,021,410	[29]	A edited the talk page of B on Wikipedia
Intra-organizational	34.	Consulting*	46	879	[17]	B turned to A for advice
	35.	Freemans-1*	34	645	[23]	A was nominated by B on a questionnaire as acquaintance
	36.	Freemans-2*	34	830	[23]	A was nominated by B on a questionnaire as acquaintance
	37.	Manufacturing*	77	2,228	[17]	B turned to A for advice
	38.	University*	81	817	[41]	A was nominated by B on a questionnaire

Table 2: Summary of the real networks analyzed in the paper. n denotes the number of nodes, m denotes the number of edges. Networks where the edges were reversed compared to the original publication are marked by an asterisk (*).

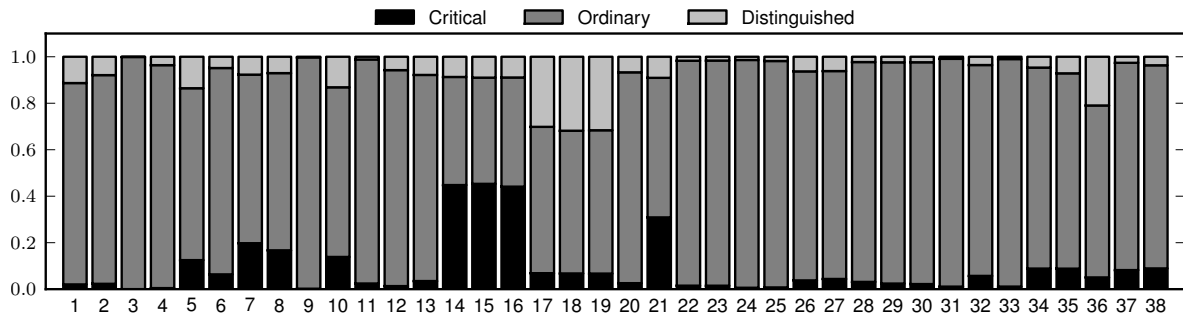


Figure 4: Fraction of distinguished (light gray), ordinary (dark gray) and critical (black) edges in the real networks studied in this paper. Numbers refer to the network indices in Table C.1.

C.3 Implementation

An open-source implementation of the driver node calculations and the edge classification for arbitrary networks is provided at <http://github.com/ntamas/netctrl>.

References

- [1] T. Achacoso and W. Yamamoto. *AY's Neuroanatomy of C. elegans for Computation*. CRC Press, Boca Raton, FL, 1st edition, 1992.
- [2] L. Adamic and N. Glance. The political blogosphere and the 2004 US election. In *Proceedings of the WWW-2005 Workshop on the Weblogging Ecosystem*. 2005.
- [3] R. Albert and A.-L. Barabási. Statistical mechanics of complex networks. *Rev. Mod. Phys.*, 74:47, 2002.
- [4] R. Albert, H. Jeong, and A.-L. Barabási. Diameter of the World Wide Web. *Nature*, 401:130–131, 1999.
- [5] R. Albert, H. Jeong, and A.-L. Barabási. Error and attack tolerance of complet networks. *Nature*, 406:378–382, 2000.
- [6] L. Amaral, A. Scala, M. Barthelémy, and H. Stanley. Classes of small-world networks. *Proc. Natl. Acad. Sci. USA*, 97:11149–11152, 2000.
- [7] S. Balaji, M. Babu, L. Iyer, N. Luscombe, and L. Aravind. Comprehensive analysis of combinatorial regulation using the transcriptional regulatory network of yeast. *J. Mol. Biol.*, 360(1):213–27, 2006.
- [8] A.-L. Barabási and R. Albert. Emergence of scaling in random networks. *Science*, 286:509–512, 1999.
- [9] G. Bianconi, N. Gulbahce, and A. Motter. Local structure of directed networks. *Phys. Rev. Lett.*, 100:118701, 2008.
- [10] G. Bianconi and M. Marsili. Loops of any size and hamilton cycles in random scale-free networks. *J. Stat. Mech.*, page P06005, 2005.

- [11] S. Boccaletti, V. Latora, Y. Moreno, M. Chavez, and D.-U. Huang. Complex networks: structure and dynamics. *Phys. Rep.*, 424(4–5):175–308, 2006.
- [12] B. Bollobás. *Random Graphs*. Cambridge Studies in Advanced Mathematics. Cambridge University Press, Cambridge, second edition, 2001.
- [13] G. Caldarelli. *Scale-Free Networks: Complex Web in Nature and Technology*. Oxford University Press, 2007.
- [14] R. Christian and J. Luczkovich. Organizing and understanding a winter’s seagrass food-web network through effective trophic levels. *Ecological Modelling*, 117:99–124, 1999.
- [15] R. Cohen, K. Erez, D. Ben-Avraham, and S. Havlin. Resilience of the Internet to random breakdowns. *Phys. Rev. Lett.*, 85:4626–4628, 2000.
- [16] N. Cowan, E. Chastain, D. Vilhena, J. Freudenberg, and C. Bergstrom. Nodal dynamics determine the controllability of complex networks, 2011.
- [17] R. Cross and A. Parker. *The Hidden Power of Social Networks*. Harvard Business School Press, Boston, MA, USA, 2004.
- [18] J. Dunne, R. Williams, and N. Martinez. Food-web structure and network theory: The role of connectance and size. *Proc. Natl. Acad. Sci. USA*, 99(20):12917–22, 2002.
- [19] H. Ebel, J. Davidsen, and S. Bornholdt. Dynamics of social networks. *Complexity*, 8:24–27, 2002.
- [20] P. Erdős and A. Rényi. On the evolution of random graphs. *Publ. Math. Inst. Hung. Acad. Sci.*, 5:17–60, 1960.
- [21] H. Fleischner. *Algorithms for Eulerian trails*, volume 50 of *Annals of Discrete Mathematics*. Elsevier, 1991.
- [22] S. Fortunato. Community detection in graphs. *Phys. Rep.*, 486:75–174, 2010.
- [23] S. Freeman and L. Freeman. Social science research reports 46. Technical report, University of California, Irvine, CA, 1979.
- [24] H. Jeong, S. Mason, A.-L. Barabási, and Z. Oltvai. Lethality and centrality in protein networks. *Nature*, 411:41–42, 2001.
- [25] H. Jeong, B. Tombor, R. Albert, Z. Oltvai, and A. Barabási. The large-scale organization of metabolic networks. *Nature*, 407(6804):651–4, 2000.
- [26] R. Kalman. Mathematical description of linear dynamical systems. *J. Soc. Indus. Appl. Math. Ser. A*, 1:152–192, 1963.
- [27] H. Kwak, C. Lee, H. Park, and S. Moon. What is Twitter, a social network or a news media? In *WWW’10: Proceedings of the 19th International Conference on World Wide Web*, pages 591–600, Raleigh, North Carolina, USA, 2010. ACM.
- [28] J. Leskovec and C. Faloutsos. Graphs over time: densification laws, shrinking diameters and possible explanations. In *Proceedings of the ACM SIGKDD International Conference on Knowledge Discovery and Data Mining (KDD)*, 2005.

- [29] J. Leskovec, D. Huttenlocher, and J. Kleinberg. Signed networks in social media. In *Proceedings of the ACM SIGCHI Conference on Human Factors in Computing Systems (CHI)*, 2010.
- [30] J. Leskovec, K. Lang, A. Dasgupta, and M. Mahoney. Community structure in large networks: natural cluster sizes and the absence of large well-defined clusters. *Internet Mathematics*, 6(1):29–123, 2009.
- [31] C. Lin. Structural controllability. *IEEE Trans. Automat. Contr.*, 19:201–8, 1974.
- [32] Y. Liu, J. Slotine, and A. Barabási. Controllability of complex networks. *Nature*, 473(7346):167–73, 2011.
- [33] A. Lombardi and M. Hörnquist. Controllability analysis of networks. *Phys Rev E*, 75:056110, 2007.
- [34] N. Luscombe, M. Madan Babu, H. Yu, M. Snyder, A. Teichmann, and M. Gerstein. Genomic analysis of regulatory network dynamics reveals large topological changes. *Nature*, 431:308–312, 2004.
- [35] N. Martinez. Artifacts or attributes? Effects of resolution on the Little Rock Lake food web. *Ecological Monographs*, 61:367–392, 1991.
- [36] R. Milo, S. Itzkovitz, N. Kashtan, R. Levitt, S. Shen-Orr, I. Ayzenshtat, M. Sheffer, and U. Alon. Superfamilies of evolved and designed networks. *Science*, 303(5663):1538–42, 2004.
- [37] R. Milo, S. Shen-Orr, S. Itzkovitz, N. Kashtan, D. Chklovskii, and U. Alon. Network motifs: simple building blocks of complex networks. *Science*, 298(5594):824–7, 2002.
- [38] K. Murota. *Systems Analysis by Graphs and Matroids*. Springer-Verlag, Berlin, 1987.
- [39] M. Nagy, Z. Ákos, D. Biro, and T. Vicsek. Hierarchical group dynamics in pigeon flocks. *Nature*, 464:890–893, 2010.
- [40] L. Négyessy, T. Nepusz, L. Kocsis, and F. Bacsó. Prediction of the main cortical areas and connections involved in the tactile function of the visual cortex by network analysis. *Eur. J. Neurosci.*, 23(7):1919–1930, 2006.
- [41] T. Nepusz, A. Petróczy, L. Négyessy, and F. Bacsó. Fuzzy communities and the concept of bridgeness in complex networks. *Phys. Rev. E*, 77:016107, 2008.
- [42] M. Newman. The structure and function of complex networks. *SIAM Rev.*, 45:167–256, 2003.
- [43] M. Newman and M. Girvan. Finding and evaluating community structure in networks. *Phys. Rev. E*, 69:026113, 2004.
- [44] M. Newman, D. Watts, and S. Strogatz. Random graph models of social networks. *Proc. Natl. Acad. Sci. USA*, 99(Suppl 1):2566–2572, 2002.

- [45] K. Norlen, G. Lucas, M. Gebbie, and J. Chuang. EVA: Extraction, visualization and analysis of the telecommunications and media ownership network. In *Proceedings of the International Telecommunications Society 14th Biennial Conference (ITS2002)*, Seoul, South Korea, August 2002.
- [46] G. Palla, A.-L. Barabási, and T. Vicsek. Quantifying social group evolution. *Nature*, 446:664–667, 2007.
- [47] G. Palla, I. Derényi, I. Farkas, and T. Vicsek. Uncovering the overlapping community structure of complex networks in nature and society. *Nature*, 435:814–818, 2005.
- [48] G. Palla, I. Farkas, P. Pollner, I. Derényi, and T. Vicsek. Directed network modules. *New J. Phys.*, 9:186, 2007.
- [49] P. Panzarasa, T. Opsahl, and K. Carley. Patterns and dynamics of users’ behaviour and interaction: Network analysis of an online community. *Journal of the American Society for Information Science and Technology*, 60(5):911–932, 2009.
- [50] R. Pastor-Satorras and A. Vespignani. Epidemic spreading in scale-free networks. *Phys. Rev. Lett.*, 86:3200–3203, 2001.
- [51] R. Pastor-Satorras and A. Vespignani. Immunization of complex networks. *Phys. Rev. E*, 65:036104, 2002.
- [52] R. Prill, P. Iglesias, and A. Levchenko. Dynamic properties of network motifs contribute to biological network organization. *PLoS Biol.*, 3(11):e343, 2005.
- [53] A. Rahmani, M. Ji, M. Mesbahi, and M. Egerstedt. Controllability of multi-agent systems from a graph-theoretic perspective. *SIAM J Contr. Optim.*, 48:162–186, 2009.
- [54] K. Reinschke and G. Wiedemann. Digraph characterization of structural controllability for linear descriptor systems. *Linear Algebra Appl.*, 266:199–217, 1997.
- [55] M. Richardson, R. Agrawal, and P. Domingos. Trust management for the semantic web. In *Proceedings of the Second International Semantic Web Conference*, 2003.
- [56] M. Ripeanu, I. Foster, and A. Iamnitchi. Mapping the Gnutella network: Properties of large-scale peer-to-peer systems and implications for system design. *IEEE Internet Computing Journal*, 6(1):50–57, 2002.
- [57] R. Shields and J. Pearson. Structural controllability of multi-input linear systems. *IEEE Trans. Automat. Contr.*, 21:203–212, 1976.
- [58] J. Skellam. The frequency distribution of the difference between two poisson variables belonging to different populations. *Journal of the Royal Statistical Society: Series A*, 109(3):296, 1946.
- [59] J.-J. Slotine and W. Li. *Applied Nonlinear Control*. Prentice-Hall, New Jersey, 1991.
- [60] E. Sontag. *Mathematical Control Theory*. Springer, New York, 1998.

- [61] M. A. J. Van Duijn, M. Huisman, F. N. Stokman, F. W. Wasseur, and E. P. H. Zeggelink. Evolution of sociology freshmen into a friendship network. *J. Math. Soc.*, 27:153–191, 2003.
- [62] D. Watts and S. Strogatz. Collective dynamics of 'small-world' networks. *Nature*, 393(6684):440–2, 1998.
- [63] W. Yu, G. Chen, and J. Lü. On pinning synchronization of complex dynamical networks. *Automatica*, 45:429–435, 2009.